Myosin A tail domain interacting protein (MTIP) localizes to the inner membrane complex of *Plasmodium* sporozoites

Lawrence W. Bergman[1,*], Karine Kaiser[4], Hisashi Fujioka[2], Isabelle Coppens[3], Thomas M. Daly[1], Sarah Fox[1], Kai Matuschewski[4], Victor Nussenzweig[4] and Stefan H. I. Kappe[4]

[1]Division of Molecular Parasitology, Department of Microbiology & Immunology, Drexel University College of Medicine, Philadelphia, PA 19129, USA
[2]Case Western Reserve University School of Medicine, Cleveland, Ohio 44106, USA
[3]Infectious Diseases Section, Department of Internal Medicine, Yale University School of Medicine, New Haven, Connecticut 06520-8022, USA
[4]Michael Heidelberger Division, Department of Pathology, New York University School of Medicine, New York, NY 10016, USA
*Author for correspondence (e-mail: lawrence.bergman@drexel.edu)

Accepted 26 September 2002
Journal of Cell Science 116, 39-49 © 2003 The Company of Biologists Ltd
doi:10.1242/jcs.00194

Summary

Apicomplexan host cell invasion and gliding motility depend on the parasite's actomyosin system located beneath the plasma membrane of invasive stages. Myosin A (MyoA), a class XIV unconventional myosin, is the motor protein. A model has been proposed to explain how the actomyosin motor operates but little is known about the components, topology and connectivity of the motor complex. Using the MyoA neck and tail domain as bait in a yeast two-hybrid screen we identified MTIP, a novel 24 kDa protein that interacts with MyoA. Deletion analysis shows that the 15 amino-acid C-terminal tail domain of MyoA, rather than the neck domain, specifically interacts with MTIP. In *Plasmodium* sporozoites MTIP localizes to the inner membrane complex (IMC), where it is found clustered with MyoA. The data support a model for apicomplexan motility and invasion in which the MyoA motor protein is associated via its tail domain with MTIP, immobilizing it at the outer IMC membrane. The head domain of the immobilized MyoA moves actin filaments that, directly or via a bridging protein, connect to the cytoplasmic domain of a transmembrane protein of the TRAP family. The actin/TRAP complex is then re-distributed by the stationary MyoA from the anterior to the posterior end of the zoite, leading to its forward movement on a substrate or to penetration of a host cell.

Key words: Plasmodium, Gliding motility, Cell invasion, Apicomplexa, MyoA

Introduction

During apicomplexan life cycles zoite stages actively invade host cells. Many zoites, including the *Plasmodium* sporozoite (Sibley et al., 1998), also display substrate-dependant locomotion called gliding motility. Gliding motility is rapid (1-10 μm/second), does not involve cilia, flagella or cytoplasmic extensions and occurs without any apparent change in zoite shape. In the early 1980s it was proposed that gliding motility and host cell invasion must involve transmembrane surface receptors that engage with either substrate ligands or host cell ligands, and that rearward redistribution of the receptor-ligand complexes would propel the zoite forward on a substrate or into a host cell (King, 1988; Russell, 1983; Russell and Sinden, 1981). In *Plasmodium* sporozoites, targeted gene disruption (Sultan et al., 1997) and site-directed mutagenesis (Kappe et al., 1999; Matuschewski et al., 2002) identified the thrombospondin-related anonymous protein (TRAP) as the transmembrane link, connecting bound extracellular ligands to the putative intracellular motor components. It is likely that the TRAP ortholog MIC2, expressed in *Toxoplasma* tachyzoites (Wan et al., 1997), and the TRAP paralog CTRP, expressed in *Plasmodium* ookinetes (Trottein et al., 1995), fulfill a similar function.

Gliding motility and invasion of host cells are inhibited by cytochalasins, which indicates that the parasites' actin filaments are required for locomotion (Dobrowolski and Sibley, 1996). In addition, the reversible myosin inhibitor butane-2,3-monoxime (BDM) blocks locomotion, which suggests that a myosin motor together with actin provides the underlying force (Dobrowolski et al., 1997a; Matuschewski et al., 2001; Pinder et al., 1998).

Apicomplexan zoites are delimited by a tri-laminar pellicle consisting of a plasma membrane and two closely aligned inner membranes that form the inner membrane complex (IMC). The cytoplasmic side of the IMC faces the subpellicular microtubule system and might be connected to it by intramembranous particles (IMPs) (Morrissette et al., 1997). Myosin and actin localize to the space between the plasma membrane and the outer membrane of the IMC in *Toxoplasma* tachyzoites (Dobrowolski et al., 1997a) and *Plasmodium* merozoites (Pinder et al., 2000). Thus the putative actomyosin motors are in the right position to power gliding motility and invasion.

The most likely candidate myosin motor is myosin A (MyoA), a class XIV unconventional myosin that is unique to the phylum Apicomplexa (Heintzelman and Schwartzman, 1997; Pinder et al., 1998). It is expressed in all *Plasmodium* invasive stages (merozoites, sporozoites and ookinetes)

(Margos et al., 2000; Matuschewski et al., 2001; Pinder et al., 1998) and also in *Toxoplasma* tachyzoites (Heintzelman and Schwartzman, 1999). Recently it was shown that MyoA is indeed essential for gliding motility and host cell invasion of *Toxoplasma* tachyzoites (Meissner et al., 2002). The MyoA head domain displays the universally conserved ATP and actin binding sites. MyoA binds actin and is released from actin in an ATP-dependant fashion (Heintzelman and Schwartzman, 1999; Hettmann et al., 2000). However, MyoA has unusual features. Its putative short neck domain has no conserved IQ motifs (consensus IQXXXRGXXXRK) that function as light chain binding sites in the neck domains of many myosins (Mooseker and Cheney, 1995). In addition, MyoA has a very short C-terminal tail domain.

In this report we attempted to identify proteins that interact with the MyoA neck and tail domains using the yeast two-hybrid system. We reasoned that MyoA-interacting proteins should be components of the apicomplexan motility and host cell invasion apparatus.

Materials and Methods

MyoA model

P. yoelii MyoA was modeled by homology, using the crystal structure of the pre-power stroke state of chicken smooth muscle myosin (Dominguez et al., 1998). An extensive Monte Carlo energy minimization was carried out in the internal coordinate space (Abagyan et al., 1997; Cardozo et al., 1995).

Plasmid construction

To construct the two hybrid bait vector containing the C-terminal 75 amino acids of *P. yoelii* MyoA, a region of *P. yoelii yoelii* 17XL genomic DNA was amplified using primers containing a 5′-*Eco*RI site and a 3′-*Pst*I site. The resulting fragment was sequenced, and cloned into the Gal4 DNA binding domain vector pAS2.1 (Clontech). A deletion of the MyoA, which removed the C-terminal 15 amino acids, was constructed as described above, except that the 3′-primer introduced a stop codon after amino acid 902. Plasmids expressing binding domain fusions containing solely the C-terminal 15 amino acids of MyoA (or mutants within that region) were constructed using synthetic oligonucleotides directly cloned in the vector pAS2.1. Deletions of MTIP were made using oligonucleotides containing either a 5′-*Eco*RI site or 3′-*Sal*I site. The resulting fragments were sequenced and subsequently cloned into the Gal4 activation domain vector pGAD424 (Clontech).

The full length MTIP gene region was amplified from *P. yoelii yoelii* 17XL genomic DNA by PCR using oligonucleotides containing a 5′-*Eco*RI site and a 3′-*Pst*I site. Following restriction endonuclease digestion, the insert was directionally cloned into the pGEX-4T-1 expression vector (Pharmacia). DNA sequencing of the insert and vector junctions confirmed an in-frame joining with the 3′ end of the *S. japonicum* GST gene. *E. coli* cells (BL21-CodonPlus-RIL, Stratagene) were transformed with the expression vector and clones expressing the fusion protein, designated GST-MTIP, were identified by immunoblot using anti-GST serum. GST-MTIP was prepared by affinity chromatography using glutathione–agarose (Sigma) (Smith and Johnson, 1988).

Yeast two-hybrid screen

The pAS2.1-MyoA vector was used to transform strain PJ69-4a and subsequently transformed with the *P. yoelii* blood stage cDNA-activation domain library essentially as previously described (Daly et al., 2001). Activation domain plasmids were rescued into *E. coli* from His^+, Ade^+ yeast colonies. Seventy-six plasmids were positive upon re-screening. The nature of these plasmids was determined either by DNA sequencing using a 5′-vector-specific activation domain primer (15 plasmids) or by PCR analysis using a primer derived from MTIP and a 3′-vector-specific primer (61 plasmids). Yeast cells containing the MyoA and MTIP constructs shown in Fig. 2 were grown in synthetic media lacking leucine and tryptophan to an OD_{600}=0.7. Cell extracts were prepared by glass bead lysis and assays performed as previously described (Bergman, 1986). The activity was normalized to the protein concentration of the extract and was expressed as nanomoles of *O*-nitrophenyl-β-D-galactoside cleaved per minute per milligram of protein.

Experimental animals and antisera

One hundred micrograms of GST-MTIP fusion protein, suspended in phosphate buffered saline, pH 7.4 (PBS), with RAS (Ribi Adjuvant System, Ribi Immunochemical Research Laboratories) was injected subcutaneously into male BALB/cByJ mice and rabbits at 3-week intervals. Two weeks after the second boost, blood was collected and serum was isolated. Polyclonal mouse anti-GST antiserum was prepared similarly. Normal mouse serum (NMS) was taken from a non-immunized BALB/cByJ mouse. The rabbit anti-MyoA antiserum was raised against a synthetic peptide (FMQLVISHEGGIRYG) corresponding to amino acids 251-265 of MyoA (Pinder et al., 1998).

Immunoblotting

Sporozoite and schizont proteins were solubilized in sample buffer and separated on 10% polyacrylamide gels. Molecular weights were verified using a prestained molecular weight marker (Biorad). Proteins were transferred to nitrocellulose (BioRad) membranes by electroblotting. Following transfer, membranes were blocked and then incubated with a 1:500 dilution of anti-MTIP antibody. Membranes were washed and then incubated for 1 hour at room temperature with a horseradish-peroxidase-conjugated secondary antibody. Membranes were washed again and immunostained proteins were visualized with enhanced chemi-luminescence detection (Pierce).

Immunofluorescence

Infected erythrocytes were spread in PBS/gelatin, fixed with methanol/acetone at –20°C and air-dried. Salivary gland sporozoites were permeabilized with 0.05% saponin and fixed with 2% paraformaldehyde. MTIP was detected with the polyclonal anti-MTIP-GST fusion protein antibody (1:1000) and FITC-conjugated goat anti-mouse IgG (1:100). For immunofluorescence staining of hepatic stages the hepatoma cell line HepG2 was infected with *P. berghei* salivary gland sporozoites and infected cells were cultured for 24 and 48 hours. Cells were permeabilized with 0.05% saponin, fixed with 2% paraformaldehyde and stained with an anti-HSP70 monoclonal antibody (Tsuji et al., 1994) and the rabbit polyclonal anti-MTIP-GST fusion protein antibody. Bound antibodies were detected using Alexa-Fluor-488- and Alexa-Fluor-594 (Molecular Probes)-conjugated anti-mouse and anti-rabbit secondary antibodies.

Electron microscopy

For transmission electron microscopy salivary glands of *P. yoelii*-infected mosquitoes were fixed with 2.5% glutaraldehyde in 0.05 M phosphate buffer, pH 7.4, with 4% sucrose for 2 hours and then postfixed in 1% osmium tetroxide for 1 hour. After a 30 minute en bloc stain with 1% aqueous uranyl acetate, the cells were dehydrated in ascending concentrations of ethanol and embedded in Epon 812. Ultrathin sections were stained with 2% uranyl acetate in 50% methanol and with lead citrate. For immunoelectron microscopy salivary glands of the *P. yoelii* infected mosquitoes were fixed for 30

minutes at 4°C with 1% formaldehyde, 0.5% glutaraldehyde in 0.1 M phosphate buffer, pH 7.4. Fixed samples were washed, dehydrated and embedded in LR White resin (Polysciences, Warrington, PA). Thin sections were treated with PBS-glycine, then blocked in PBS containing 1% w/v bovine serum albumin (BSA) and 0.01% v/v Tween 20 (PBTB). Grids were then incubated with primary antibodies (anti-MTIP or anti-MyoA) diluted 1:50 ~1:500 in PBTB for 2 hours at room temperature. Negative controls included normal Mouse or rabbit serum and PBTM applied as the primary antibody. After washing, grids were incubated for 1 hour in the gold-conjugated goat anti-mouse or -rabbit IgG (Amersham Life Sciences, Arlington, IL) diluted 1:20 in PBTB, rinsed with PBTB, and fixed with glutaraldehyde to stabilize the gold particles. Samples were stained with uranyl acetate and lead citrate, and then examined in a Zeiss CEM902 electron microscope. For cryo-immunoelectron microscopy salivary glands of the *P. yoelii* infected mosquitoes were fixed for 2 days at 4°C with 8% paraformaldehyde. Infected glands were infiltrated, frozen, sectioned and labeled as described (Folsch et al., 2001) with the difference that rabbit anti-MTIP polyclonal antibody was used (1:200 in PBS/1% fish skin gelatin), followed directly by 10 nm protein A gold.

Membrane extraction

P. yoelii salivary gland sporozoites (6×10^5) were suspended in PBS containing 1% Triton X-100 (TX-100) and incubated on ice for 30 minutes. The preparation was centrifuged at 13,800 ***g*** for 20 minutes at 4°C to separate the TX-100 soluble (plasma membrane) from the insoluble (IMC) fraction. The pellet was washed three times in PBS. Untreated sporozoites or the total pellet and total supernatant of TX-100-treated sporozoites were suspended in sample buffer and separated on 10% polyacrylamide gels. Proteins were transferred to nitrocellulose (BioRad) membranes by electroblotting. Following transfer, membranes were blocked and then incubated with a 1:1000 dilution of anti-MTIP antibody or a 1:1000 dilution of a monoclonal anti-*P. yoelii* CS antibody. Membranes were washed and then incubated for 1 hour at room temperature with a horseradish-peroxidase-conjugated secondary antibody. Membranes were washed again and immunostained proteins were visualized with enhanced chemiluminescence detection (Pierce).

For immunofluorescence, sporozoites were treated for 30 minutes on ice with 1% TX-100 in PBS, washed three times in PBS and fixed for 10 minutes in 2% of paraformaldehyde in PBS at room temperature. Treated and untreated sporozoites were incubated for 1 hour with anti-CS and anti-MTIP both diluted in 1:1000 in PBS-1% FCS. Bound antibodies were detected using Alexa Fluor 488 and Alexa Fluor 594 (Molecular Probes) conjugated anti-mouse and anti-rabbit secondary antibodies. Relative fluorescence intensities were quantified using the MetaMorph imaging system (Universal Imaging Corporation). Measurements were taken from 50 TX-100-treated and 50 untreated sporozoites. Exposure times were kept constant between individual measurements.

Results

Identification of a MyoA-interacting protein

To detect proteins that interact with the presumptive neck and tail domains of MyoA (Fig. 1A) we used the yeast two-hybrid system. The C-terminal 75 amino acids of MyoA of

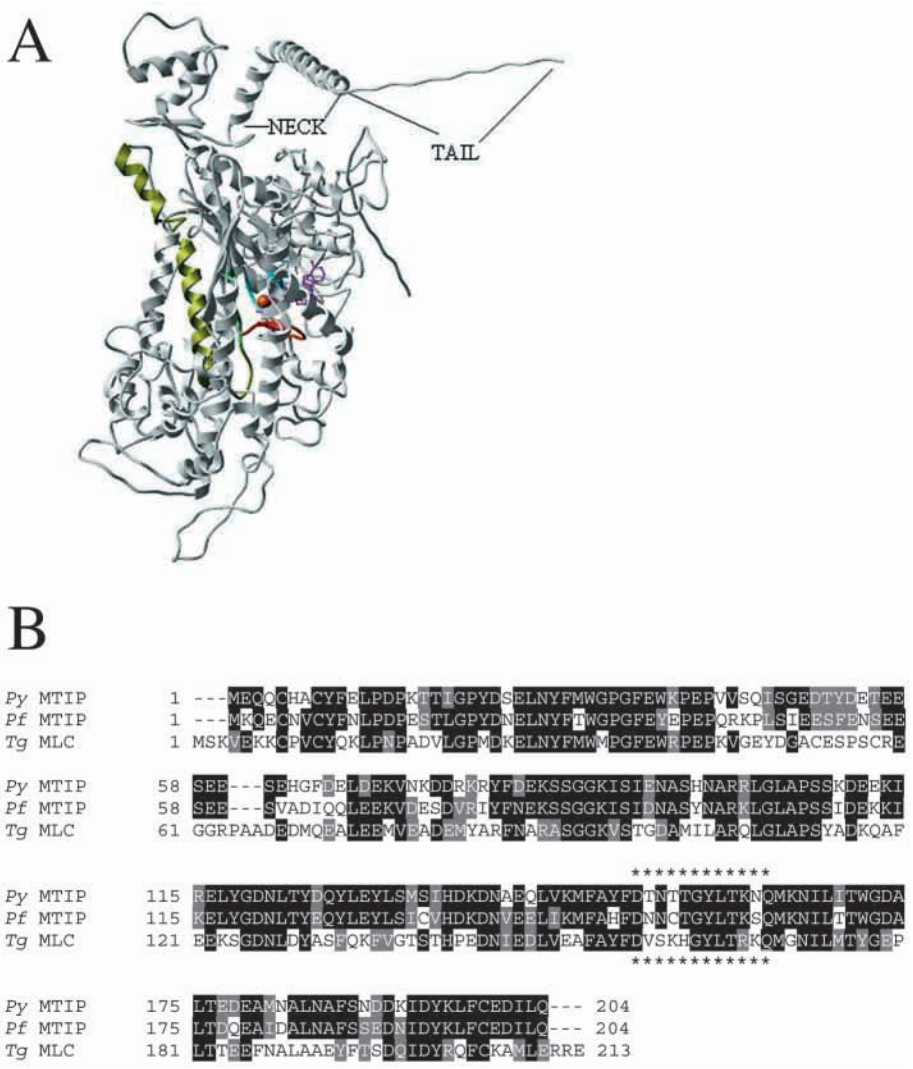

Fig. 1. (A) Predicted tertiary structure of *P. yoelii* MyoA based on the crystal structure of chicken smooth muscle myosin. The ATP-binding pocket is shown with a bound ATP analog. The MyoA primary amino acid sequence corresponding to the neck domain is predicted to form an α-helix. (B) Amino acid sequence alignment of *P. yoelii* (Py) MTIP, the MTIP ortholog from *P. falciparum*(Pf), obtained by BLAST analysis of the *P. falciparum* genome sequence information (Stanford_Chr12Contig01.010524, nucleotides 1931214-1031825) and the putative myosin light chain of *T. gondii* (Tg) (accession no. AY048862). The putative EF hand motif is indicated by asterisks. Identical amino acid residues are shown in white letters on black. Conserved amino acid changes are shown as white letters on gray. Radical amino acid changes are shown as black letters. The *P. yoelii* MTIP sequence is available from GenBank/EMBL/DDBJ under accession no. AF465245.

Plasmodium yoelii (PyMyoA) were fused to the DNA binding domain of the yeast Gal4 molecule. This bait was used to screen 1.1×10^6 transformants of an activation domain-cDNA library, derived from mRNA isolated from a mixed blood stage infection of *P. yoelii* 17XL (Daly et al., 2001). Seventy-six plasmids were isolated that were positive after two rounds of screening and all contained inserts that matched a single open reading frame on a contig in the *P. yoelii* genome sequence database (www.tigr.org). Analysis of this open reading frame predicted a putative protein of 24 kDa (Fig. 1B). A search of the *P. falciparum* genome sequence database (http://PlasmoDB.org) identified a gene on chromosome 12 encoding a protein of identical size with 69% amino acid sequence identity to the *P. yoelii* protein (Fig. 1B). A BLASTP search of the non-redundant sequence database at NCBI showed highest identity (43%) of the *P. yoelii* and *P. falciparum* proteins to a *T. gondii* protein (aligned in Fig. 1B) annotated as a myosin light chain (TgMLC1) (Herm-Gotz et al., 2002), and showed much lower identity (23%) to calmodulin. We named the protein MyoA tail domain interacting protein, MTIP (see below). Modular architecture research tool analysis (smart.embl-heidelberg.de) revealed a single 12 amino acid motif within the *Plasmodium* and the *Toxoplasma* MTIPs with similarity to EF-hand Ca^{2+} binding domains.

MTIP binds to the tail domain of MyoA

To further map the part of MyoA that is critical for binding to MTIP we constructed DNA binding domain vectors that contain solely the presumptive α-helical neck domain of MyoA (residues 842-902 of the full length molecule) or the 15 amino acid tail domain (residues 903-917). Surprisingly, not the neck domain but the 15 amino acid tail domain was necessary and sufficient for the MyoA interaction as measured qualitatively using growth in the absence of adenine or histidine or quantitatively measuring interaction-dependent expression of an integrated GAL1-LacZ fusion (Fig. 2A).

Next we asked which region of MTIP is involved in the interaction with the MyoA tail domain. The minimal interacting region of MTIP isolated from the original library screen encompassed residues 80-204 (Fig. 2B). We removed additional 15 amino acids from the N-terminal end of the minimal interacting region (residues 80-94) and this deletion eliminated the ability of MTIP to interact with the MyoA tail domain. Removal of 15 C-terminal amino acids (residues 190-204) also eliminated the interaction. Therefore the entire 79-204 MTIP region may be required for the interaction with MyoA. Alternatively, the binding site could be composed of two separate regions (residues 80-94 and 190-204) in MTIP. A previous study implicated the tail domain of *T. gondii* MyoA (TgMyoA) in its targeting to the tachyzoite periphery, presumably the plasma membrane. Mutagenesis of a dibasic motif within the tail of TgMyoA abolished localization to the periphery (Hettmann et al., 2000). We made the analogous mutations in the tail of PyMyoA and found that these changes abolished the interaction of the PyMyoA tail domain with MTIP (Fig. 2C).

MTIP is expressed in invasive stages of *Plasmodium*

We examined the expression pattern of transcripts encoding MTIP using cDNA blots and reverse transcriptase-PCR. *MTIP* was expressed in blood stage parasites and sporozoites of *P. yoelii* (data not shown). To localize MTIP, we expressed and purified a GST-MTIP fusion protein. Both a polyclonal mouse antiserum and a polyclonal rabbit antiserum directed against the fusion protein specifically recognized MTIP released by thrombin cleavage of the GST-MTIP fusion in western blots,

A.

Clone	Amino Acids	Interaction with pAD-MTIP	β-Galactosidase Activity[a]
pAS2.1-MYOA			
◆——◆	842-917	+ + +	97.9 ±4.5
◆——●	842-902	-	5.8 ±2.0
●—◆	903-917	+ + +	107.3 ±5.0

B.

pAD-MTIP		pAS2.1-MYOA	
◆——◆	1-204	+ + +	100.0 ±5.1
●——◆	80-204	+ + +	132.8 ±5.9
●—◆	95-204	-	5.2 ±1.9
◆——●	1-189	-	7.2 ±1.8

C.

pAS2.1-		pAD-MTIP	
MyoA Tail	-RVQAHIRKRMVA	+ + +	116.2 ±3.2
Mutant 2A	-RVQAHIAARMVA	-	5.8 ±1.5
Mutant 3A	-TVQAHIAAAMVA	-	5.7 ±1.0

Fig. 2. Localization of regions involved in MyoA and MTIP interaction. (A) The putative neck (amino acids 842-902) and tail (amino acids 903-917) domains of *P. yoelii* MyoA were cloned together or separately into the Gal4 DNA binding domain vector pAS2.1. The resulting plasmids were transformed into yeast strain PJ69-4a, containing the full length *P. yoelii* MTIP in the Gal4 activation domain vector (pAD-MTIP), and assayed for their ability to grow in the absence of histidine or adenine (growth is indicated as +; no growth as –). Only the tail domain of MyoA was necessary and sufficient for interaction with MTIP. (B) N- and C-terminal deletions of *P. yoelii* MTIP were constructed in the Gal4 activation domain vector, transformed into yeast strain PJ69-4a containing pAS2.1-MyoA (amino acids 842-917) and assayed as described above. The minimal interacting region located to amino acids 80-204. Further N-terminal deletion of 15 amino acids or C-terminal deletion of 15 amino acids abrogated interaction. (C) Site-directed mutagenesis of the basic motif within the tail of *P. yoelii* MyoA in the vector pAS2.1-MyoA. Plasmids were analyzed as described in A. Change of RKR→AAA or RKR→AAR abrogated interaction. *Values for β-galactosidase activity are the mean of three independent cultures assayed in duplicate±s.d.

whereas a mouse polyclonal anti-GST antiserum recognized only the GST moiety (data not shown). Western analysis of total protein isolated from sporozoites or a schizont enriched fraction of blood stage parasites revealed a band of approximately 25 kDa (Fig. 3A) in both parasite stages. The protein ran as a closely migrating doublet, indicating that MTIP may be subject to proteolytic processing or post-translational modifications. MTIP contains multiple consensus serine and threonine phosphorylation sites making it possible that MTIP function is regulated by phosphorylation.

Indirect immunofluorescence assay (IFA) showed that MTIP is concentrated around the periphery of merozoites during the late stages of schizogony (Fig. 3B). In sporozoites (Fig. 3C) MTIP showed strong peripheral staining of the sporozoite with varying intensity.

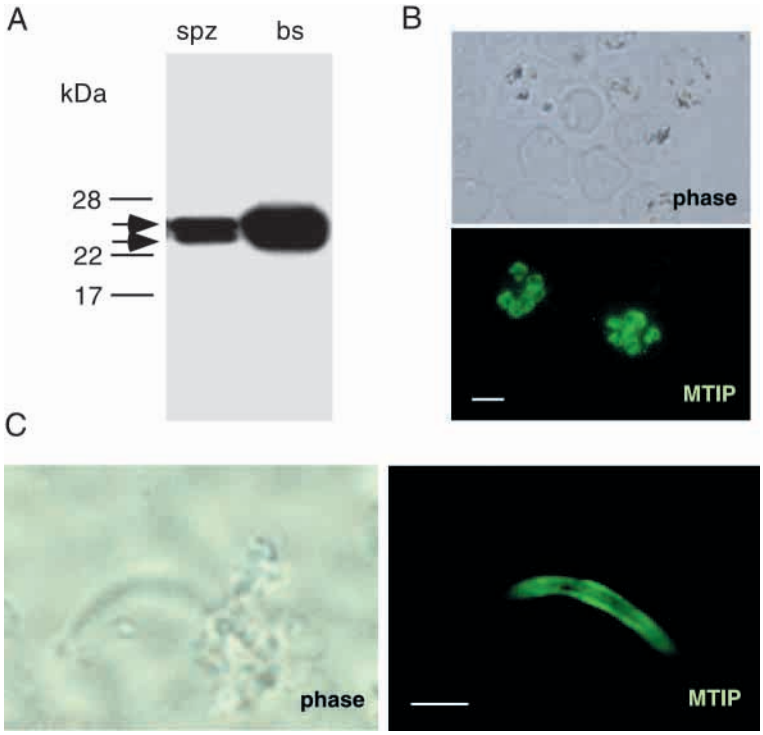

Fig. 3. MTIP is expressed in invasive *Plasmodium* zoite stages. (A) Western blot analysis of *P. yoelii* sporozoite extracts (spz) and of extracts from a schizont-enriched fraction of *P. yoelii* blood stages (bs). The anti-MTIP antiserum specifically recognized a protein doublet in both zoite preparations that closely migrated at approximately 25 kDa. (B) Indirect immunofluorescence assay (IFA) with anti-MTIP antiserum showed that MTIP is concentrated around the periphery of merozoites during the late stages of blood stage schizogony (Bar, 2 μm). (C) IFA with anti-MTIP showed strong peripheral fluorescence in *P. yoelii* sporozoites that were isolated from mosquito salivary glands (Bar, 2 μm).

MTIP localizes to the inner membrane complex of *Plasmodium* sporozoites

In transmission electron microscopy *P. yoelii* sporozoites showed the typical tri-laminar pellicle consisting of a plasma membrane and two inner membranes that form the IMC (Fig. 4A). We investigated the localization of MTIP in sporozoites by immunoelectron microscopy (Fig. 4B-D). Labeling of sections with anti-MTIP (15 nm gold particles) localized the protein to the periphery of sporozoites. Almost no labeling was observed in the internal cytoplasm (Fig. 4B). The gold particles decorated a circumferential electron dense structure that was positioned ≈15 nm underneath the outer boundary of the sporozoite, the presumed plasma membrane. We interpreted this electron dense structure as the IMC, which extends ≈15 nm underneath the plasma membrane (Fig. 4A,B). Double labeling of sections with anti-MyoA (5 nm gold particles) and anti-MTIP (15 nm gold particles) localized both proteins to the periphery of sporozoites (Fig. 4C,D). The MyoA localization was similar to that previously described for *Toxoplasma* tachyzoites and *Plasmodium* merozoites (Dobrowolski et al., 1997a; Pinder et al., 1998). Frequently MyoA was found clustered with MTIP (Fig. 4C,D). Next we used cryo sections of salivary gland sporozoites to assign MTIP more clearly to a particular membrane compartment. Labeling with anti-MTIP (10 nm gold particles) localized MTIP to the IMC and also to the cortical space between the IMC and the plasma membrane (Fig. 4E,F). The IMC of apicomplexan zoites terminates at the apical prominence, leaving the extreme apical prominence covered by the plasma membrane only. No MTIP labeling was found at the extreme prominence of sporozoites (Fig. 4F, inset).

To confirm the potential IMC localization of MTIP we made use of the differential solubility characteristics of the apicomplexan plasma membrane and IMC. Treatment with the non-ionic detergent Triton X-100 (TX-100) removes the plasma membrane and its associated proteins of *Toxoplasma* tachyzoites quantitatively; however, the IMC and associated proteins are relatively resistant to TX-100 treatment (Mann and Beckers, 2001). We subjected sporozoites to the same treatment and then used the rabbit anti-MTIP antisera for detection by IFA and immunoblots. As a control for plasma membrane localization we used a monoclonal antibody specific for the *P. yoelii* circumsporozoite (CS) protein (Ak et al., 1993). CS is the major surface protein of sporozoites presumably linked to the plasma membrane by a glycosylphosphatydilinositol (GPI) anchor (Nussenzweig and Nussenzweig, 1985). Untreated sporozoites showed uniform peripheral distribution of MTIP and CS with a notable absence of MTIP staining at one pole of the sporozoite (Fig. 5A). TX-100-treated sporozoites showed no significant changes in the linear, circumferential MTIP staining when compared with untreated sporozoites. However, TX-100-treated sporozoites showed complete loss of the peripheral CS staining. This finding was substantiated by quantitative analysis of fluorescent intensities showing no significant loss of MTIP fluorescence in TX-100 treated sporozoites but a 90% decrease of CS fluorescence (Fig. 5B). Immunoblot analysis confirmed the IFA results (Fig. 5C). TX-100-treated sporozoites retained most MTIP in the insoluble pellet fraction after high-speed centrifugation, while CS showed an inverse distribution with most protein found in the soluble supernatant fraction.

Sporozoites invade hepatocytes and transform into hepatic trophozoites. We followed MTIP localization in intracellular

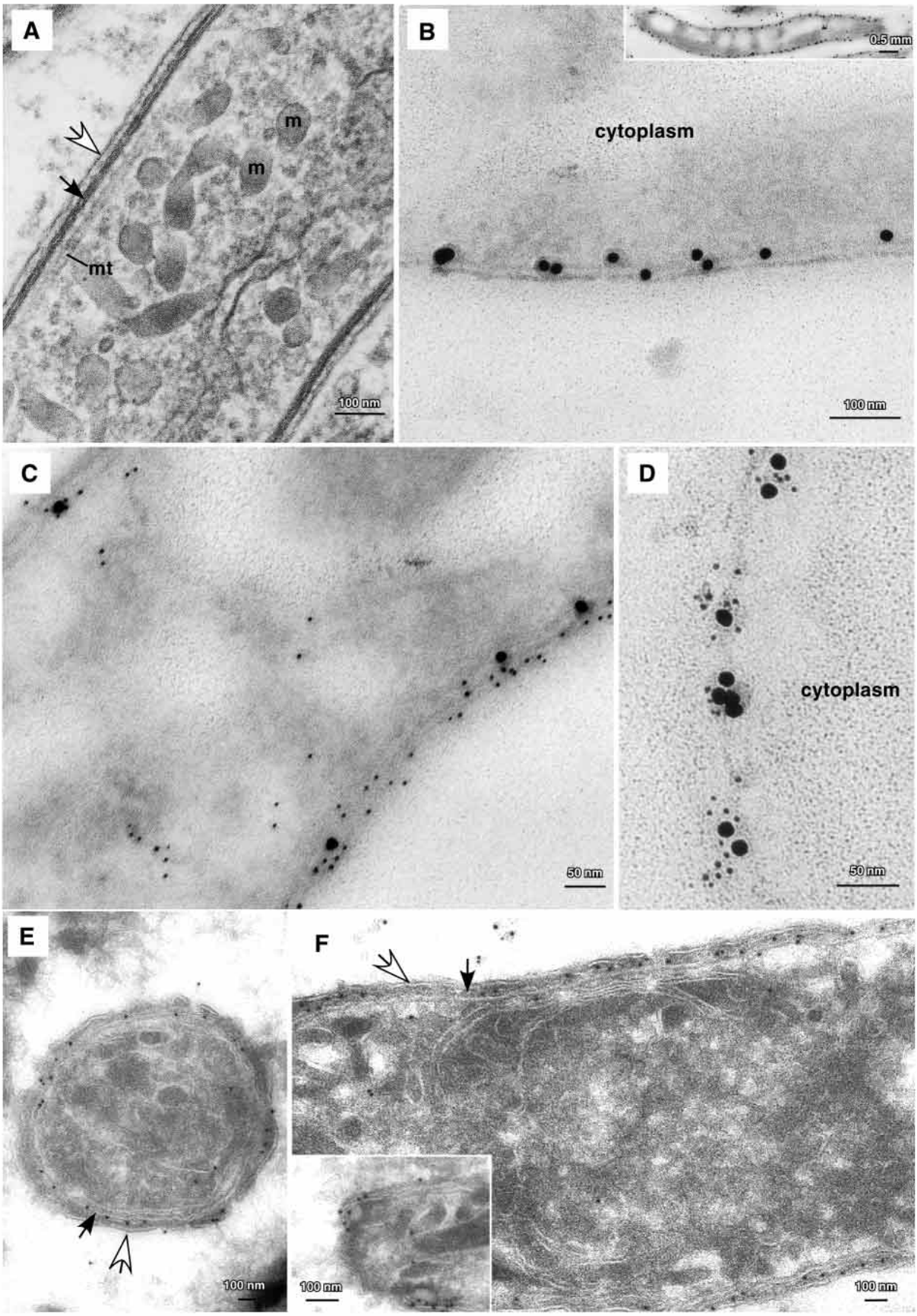
A
m
m
mt
100 nm
B
0.5 mm
cytoplasm
100 nm
C
50 nm
D
cytoplasm
50 nm
E
100 nm
F
100 nm
100 nm

Fig. 4. MTIP localizes to the inner membrane complex of *Plasmodium* sporozoites and co-localizes with MyoA. (A) The transmission electron micrograph of a longitudinal sporozoite section shows the architecture of the sporozoite cortex. The trilaminar pellicle consists of the plasma membrane (white arrow) and the IMC (black arrow) separated by the cortical cytoplasm. m, micronemes; mt, microtubules. (B) Immunoelectron microscopy of sporozoite sections labeled with anti-MTIP (15 nm gold particles). MTIP localized to the periphery of sporozoites and showed circumferential distribution. Almost no labeling was observed in the internal cytoplasm. The gold particles decorated an electron dense structure located ≈15 nm internal to the presumed plasma membrane. The position of gold particles is consistent with an IMC localization of MTIP. (C,D) Sporozoite sections double-labeled with anti-MyoA (5 nm gold particles) and anti-MTIP (15 nm gold particles) localized both proteins to the periphery of the sporozoite. MTIP was frequently clustered with MyoA. (E,F) Cryo-immunoelectron microscopy localized MTIP (10 nm gold particles) to the inner membrane complex and cortical cytoplasm of sporozoites. Note the absence of plasma membrane and the persistence of MTIP labeling in some positions. The white arrow indicates the plasma membrane; the black arrow indicates the IMC. The inset in F shows the apical prominence of a sporozoite. No gold particles label the prominence beyond the termination points of the IMC.

parasites by IFA using the hepatoma cell line HepG2 as host cells (Fig. 6). The transformation of intracellular sporozoites into hepatic trophozoites is marked by the development of a bulbous enlargement and an increase in heat shock protein 70 (HSP70) expression (Fig. 6A). In early trophozoites MTIP localized to the parasites' periphery showing an apparently uninterrupted, circumferential pattern (Fig. 6B). MTIP signal was progressively lost in later stage parasites (Fig. 6C,D) and was not detectable at 48 hours post invasion. The pattern we observed for MTIP loss in hepatic stages reflected closely the progressive disassembly of the IMC that was previously described using electron microscopy (Meis et al., 1985).

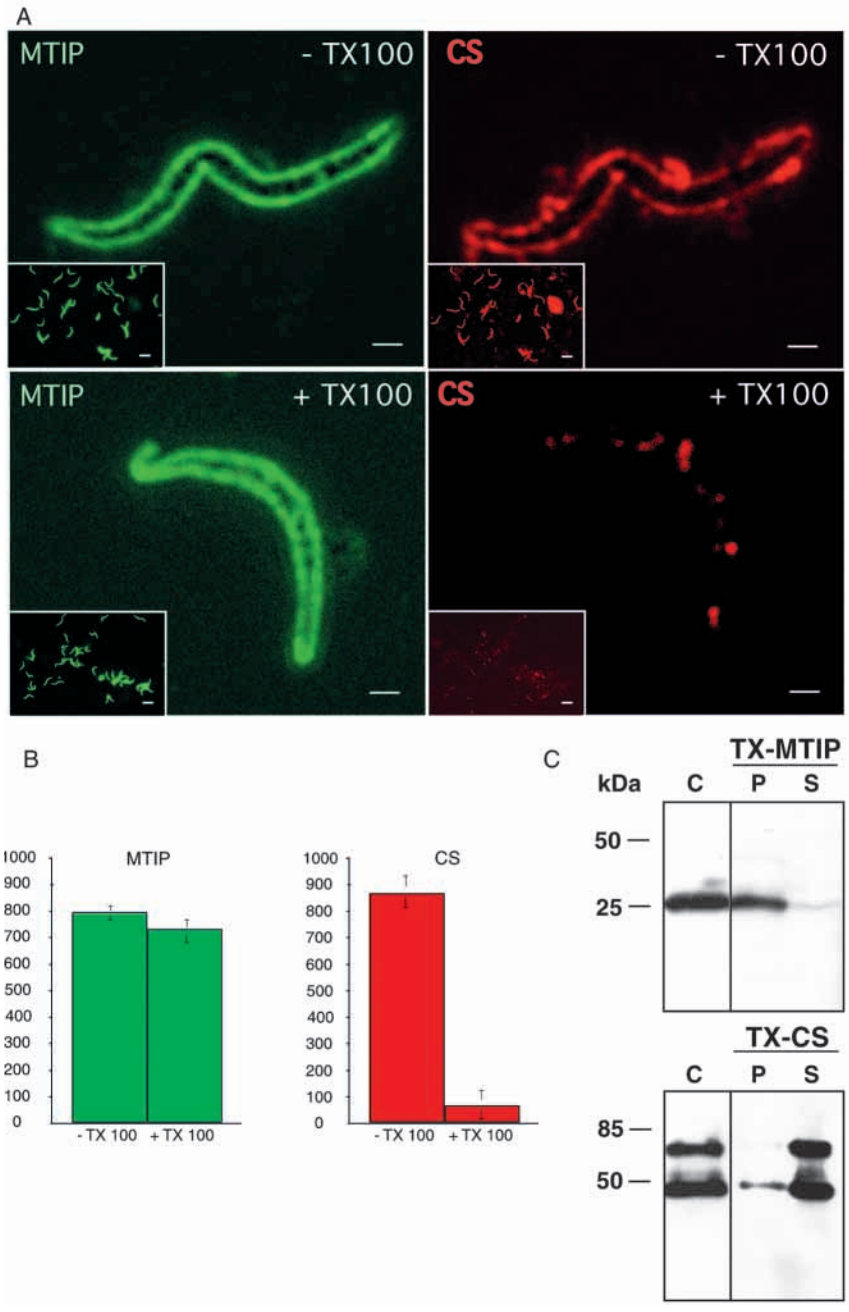

Fig. 5. Extraction of MTIP and CS with Triton X-100 (TX-100). (A) Sporozoites were permeabilized with saponin and fixed with paraformaldehyde (PFA) (upper panel, –TX100) or treated with 1% TX-100 followed by PFA fixation (lower panel, +TX100). Each preparation was labeled with anti-CS (red) and anti-MTIP (green) antibodies. In untreated sporozoites MTIP and CS were localized to the periphery of sporozoites and showed a relatively homogenous distribution. TX-100-treated sporozoites showed no significant change in MTIP distribution or fluorescent intensity. However, CS fluorescence was lost from the periphery of sporozoites by TX-100 treatment, indicating a complete removal of the plasma membrane. The inset in each panel shows overview fluorescence micrographs for each sporozoite preparation at lower magnification. Left and right panels show the same sporozoites labeled with MTIP (left panels) and CS (right panels). Scale bars are 0.5 μm for individual sporozoite micrographs and 10 μm for overview micrographs. (B) Quantification of MTIP and CS fluorescence shown in A. Graphs are the mean of relative fluorescent intensities measured on 50 sporozoites for each the TX-100-treated and untreated populations with constant exposure times±s.d. (C) Immunoblot analysis of TX-100-treated sporozoites with anti-MTIP and anti-CS antibodies. Pellet (P) and supernatant (S) were separated by high speed centrifugation and analyzed by SDS-PAGE followed by blotting and probing with anti-MTIP (upper panel) or anti-CS (lower panel). Most CS was detected in the supernatant, indicating effective solubilization of the sporozoite plasma membrane and associated proteins. However, most MTIP was detected in the pellet, indicating its retention in the IMC. Total parasite extracts are shown for comparison (C). Note that CS was detected as 40/60 kDa species.

Taken together, the IEM localization, the TX-100 solubility characteristics and the pattern of loss in hepatic stages strongly support an association of MTIP with the sporozoite IMC and not the plasma membrane.

Discussion

Previous work indicated that MyoA is the myosin motor driving apicomplexan gliding motility and invasion (Heintzelman and Schwartzman, 1999; Pinder et al., 1998). A recent study finally demonstrated the central role of MyoA in *Toxoplasma* tachyzoite gliding motility and host cell infection using a modified tetracycline-inducible expression system (Meissner et al., 2002).

However, neither the MyoA cargo nor accessory molecules that regulate its activity, such as light chains, had been identified. In many myosins, the cargo interacts with the tail domain and light chains bind to the IQ motifs in the neck domain (Mermall et al., 1998). These neck and tail domains of MyoA are strikingly distinct. Similar to other myosins, the putative neck domain of MyoA is predicted to form an extended α-helix but it lacks consensus IQ motifs. We did not identify any molecule that interacts with the neck domain in the yeast two-hybrid screen. The MyoA tail is unusually short, apparently formed by the C-terminal 15 amino acids. Our results show that it is the tail of MyoA that specifically interacts with MTIP. Therefore, MTIP is integral to the motor complex. MTIP is distantly related to myosin light chains and might function as a regulatory or essential light chain for MyoA. However, its single EF-hand motif is unusual since EF-hands almost always occur in pairs, presumably to stabilize the protein conformation and to act cooperatively in the binding of Ca^{2+} (Nelson and Chazin, 1998). We cannot exclude the possibility that MTIP dimerizes bringing two EF-hands together. EF-hands consist of a helix-loop-helix structure where the loop coordinates the metal. The calcium ion is coordinated in a pentagonal bipyramidal configuration. The six residues involved in the binding are in positions 1, 3, 5, 7, 9 and 12 of the loop with an invariant glutamate or aspartate at position 12 (Lewit-Bentley and Rety, 2000). Secondary structure prediction indicated that the EF-hand motif of MTIP forms a helix-loop-helix structure; however, the residue at position 12 is a glutamine, making it unlikely that this motif coordinates Ca^{2+} at physiological concentrations. However, EF-hand-containing proteins can also exhibit Ca^{2+}-independent binding to targets. Thus the functional properties of the MTIP EF-hand motif remain to be elucidated by site-directed mutagenesis and Ca^{2+}-binding assays.

In a previous study it was shown that the tail domain of TgMyoA was essential for targeting the protein to the tachyzoite periphery (Hettmann et al., 2000) and that mutagenesis of a conserved dibasic motif within the tail abolished correct localization. Here we showed that mutagenesis of the dibasic motif in the *Plasmodium* MyoA tail domain abolished interaction with MTIP. It is therefore likely that, in the *Toxoplasma* study, it was the *T. gondii* MTIP

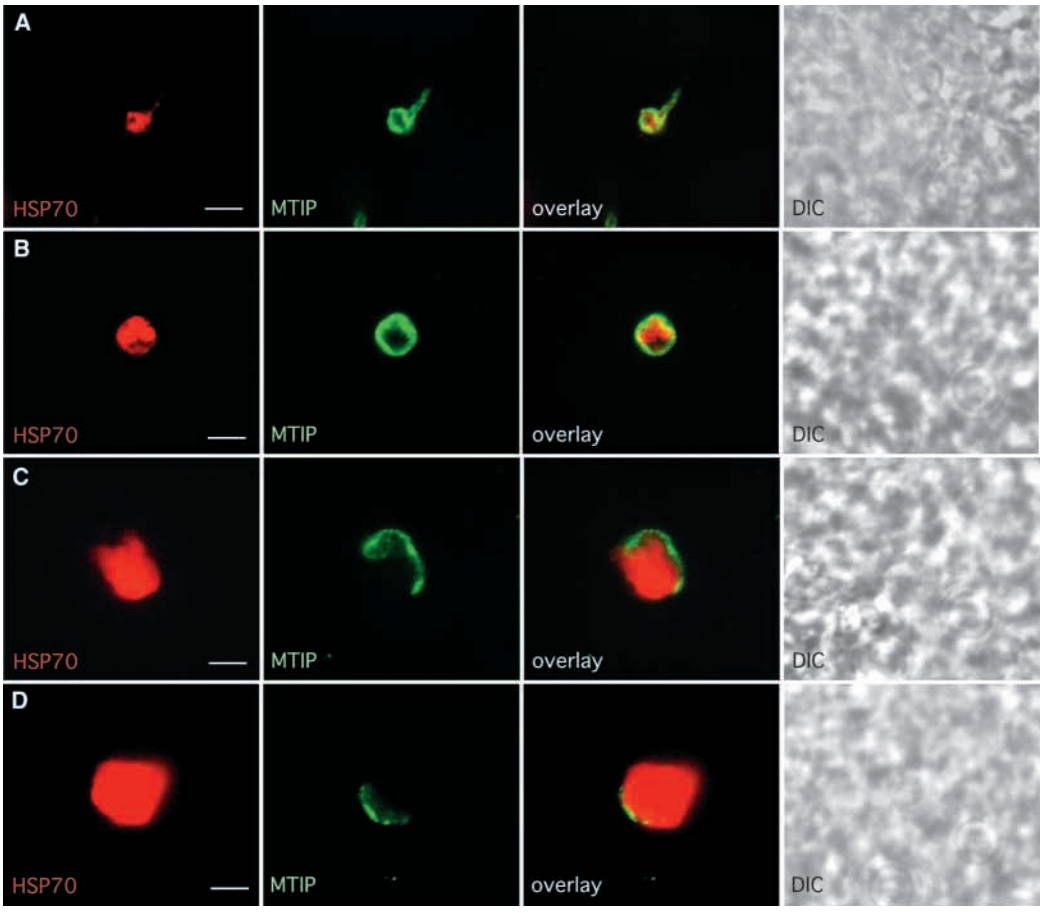

Fig. 6. MTIP is progressively lost during development of hepatic stages, reflecting the disassembly of the inner membrane complex (IMC). (A) Early hepatic trophozoite stage showing a typical transformation bulb. Heat shock protein 70, which is not significantly expressed in sporozoites shows increase of expression. (B) A spherical hepatic trophozoite (24 hours after invasion) shows still complete circumferential MTIP staining. (C,D) Later stage hepatic stages (36-45 hours after invasion) show progressive loss of MTIP staining closely resembling the progressive loss of the IMC during these stages of development (Meis et al., 1985). DIC, differential interference contrast.

ortholog that localized MyoA to the tachyzoite periphery. Indeed, concurrent with our findings, the MTIP ortholog of *Toxoplasma* (TgMLC1) was identified (Herm-Gotz et al., 2002). This study also demonstrated an association of TgMLC1 with TgMyoA using biochemical assays. Taken together our results and previous studies thus indicate that MTIP/MLC1 acts as a cargo for MyoA and suggest that their interactions determine IMC localization of MyoA. MTIP might also regulate MyoA motor activity, but no available experimental data support such a function.

By immunoelectron microscopy MTIP showed a distribution consistent with its residence in the IMC. IMC association of MTIP was also supported by its solubility characteristics in TX-100-treated sporozoites. In addition, MTIP is lost during development of hepatic stages in a spatio-temporal pattern that was consistent with its IMC association. Finally, MTIP is absent at the extreme apical prominence of sporozoites, which reflects the absence of IMC at this position. This has also been shown for TgMLC1/MTIP (Herm-Gotz et al., 2002). Since the MTIP amino acid sequence does not predict transmembrane domains or lipid attachment sites it might bind to a yet unidentified protein anchored in the IMC.

The localization of MTIP has important implications for the topology of the linear actomyosin motor that powers invasion and motility in apicomplexan parasites. The prevailing model (Fig. 7A) of the motor complex assumed that a transmembrane protein (now known to be a protein of the TRAP family) is linked by its cytoplasmic domain directly or indirectly with the myosin motor (King, 1988; Pinder et al., 1998). In this model filamentous actin remains stationary, tethered to the outer membrane of the IMC by a hypothetical protein and the myosin/TRAP complex moves along those filaments. Our results favor an opposing model of motor complex configuration that is also mentioned by Pinder et al. (Fig. 7B). The localization of MTIP to the IMC suggests that it is the MTIP/MyoA complex that remains stationary tethered to the outer membrane of the IMC by an unidentified protein. This model predicts that actin, directly or indirectly connected to the

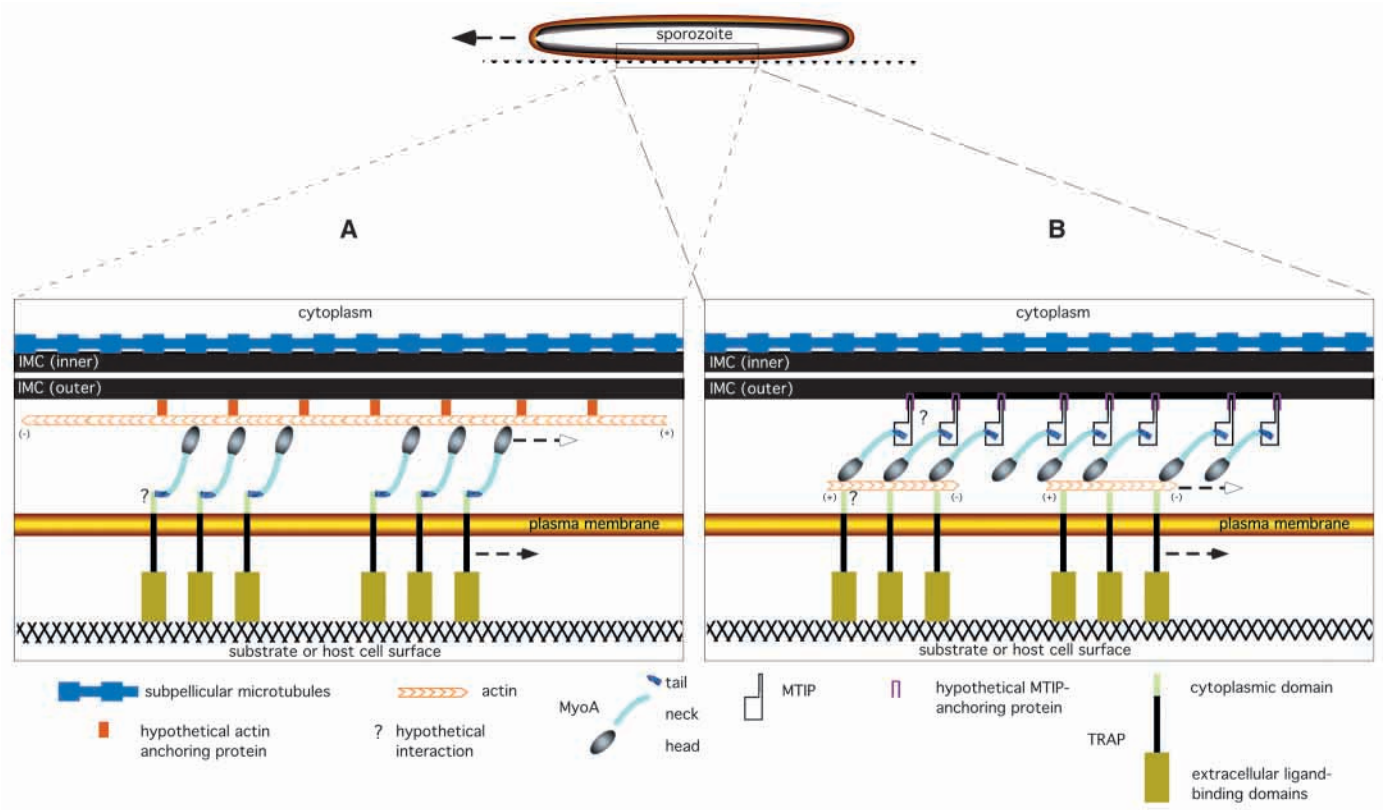

Fig. 7. Two models of the molecular motility machinery in apicomplexan zoites. The diagrams show the periphery of a *Plasmodium* sporozoite and the possible arrangements of identified and hypothetical intracellular components of the motor complex. (A) In the currently prevailing model, actin filaments are tethered to the outer membrane of the IMC by a hypothetical protein. The cytoplasmic domain of TRAP directly or indirectly interacts with the tail of MyoA. The MyoA head domain interacts with actin filaments and moves towards the plus end of the filaments. This leads to displacement of the MyoA/TRAP complex from anterior to posterior and results in a forward movement of the zoite. (B) In the alternative model the N-terminal portion of MTIP anchors it to the outer membrane of the IMC by interaction with a hypothetical protein at the IMC. MTIP binds the tail domain of MyoA, immobilizing it, and this determines MyoA orientation with the head domain projecting outward. The head domain interacts with short actin filaments that are directly or indirectly linked to the cytoplasmic domain of TRAP. The MyoA head domain interacts with actin filaments and moves towards the plus end. Because MyoA is fixed to the IMC, the actin/TRAP complex is displaced from anterior to posterior resulting in a forward movement of the zoite. Note that in model A, the plus end of the actin filaments is oriented towards the posterior of the zoite. In model B the plus end of the actin filaments is oriented towards the anterior end of the zoite. IMC, inner membrane complex; MTIP, MyoA tail domain interacting protein; MyoA, myosin A; TRAP, thrombospondin-related anonymous protein.

cytoplasmic domain of TRAP, is then moved along this complex. Indeed, recent work identified aldolase as a protein that interacts with the *T. gondii* MIC2 cytoplasmic domain and *P. falciparum* TRAP cytoplasmic domain (D. Sibley, personal communication). It is well established that aldolase of mammalian cells interacts with the actin cytoskeleton (Kusakabe et al., 1997; Schindler et al., 2001). Hence, aldolase is probably the bridge linking the cytoplasmic domains of TRAP-like proteins to the parasites' actin filaments.

The model also predicts that short actin filaments that are nucleated at the anterior end of the zoite form a complex with the cytoplasmic domain of TRAP and, after redistribution, this complex is disassembled at the posterior end. In agreement with this prediction, only ≈5% of total actin was assembled in filaments in *T. gondii* tachyzoites (Dobrowolski et al., 1997b; Poupel and Tardieux, 1999). Furthermore, when tachyzoites are treated with jasplakinolide, an actin-polymerizing and filament-stabilizing drug, actin filaments are mainly observed at the apical end (Shaw and Tilney, 1999), which might indicate the preferential localization of parasite actin polymerization factors in this region.

Whatever the topology of the motor complex, the MyoA/MTIP interaction could be essential for the function of the parasite motor. The yeast system is well poised to approach the isolation of molecules that may disrupt the interaction between these two molecules and thus may block the motility and/or invasion of malarial and other apicomplexan parasites.

We thank Matthieu Schapira for expert assistance with the MyoA model. We are grateful to Jennifer Pinder for providing us with the MyoA antisera and Moriya Tsuji for the anti-HSP70 monoclonal antibody. We wish to thank the scientists and funding agencies comprising the international Malaria Genome Project for making sequence data from the genome of *P. falciparum* (3D7) public prior to publication of the completed sequence. The Institute for Genomic Research, along with the Naval Medical Research Center (USA), sequenced *P. yoelii*. The Stanford Genome Technology Center (USA) sequenced chromosome 12, with support from the Burroughs Wellcome Fund. This work was supported by grants from the Deutsche Forschungsgemeinschaft to K.M., the National Institute of Health to V.N. and L.W.B., and a B. Levine fellowship in malaria vaccinology to S.H.I.K.

References

Abagyan, R., Batalov, S., Cardozo, T., Totrov, M., Webber, J. and Zhou, Y. (1997). Homology modeling with internal coordinate mechanics: deformation zone mapping and improvements of models via conformational search. *Proteins* **Suppl. 1**, 29-37.

Ak, M., Bower, J. H., Hoffman, S. L., Sedegah, M., Lees, A., Carter, M., Beaudoin, R. L. and Charoenvit, Y. (1993). Monoclonal antibodies of three different immunoglobulin G isotypes produced by immunization with a synthetic peptide or native protein protect mice against challenge with *Plasmodium yoelii* sporozoites. *Infect. Immun.* **61**, 2493-2497.

Bergman, L. W. (1986). A DNA fragment containing the upstream activator sequence determines nucleosome positioning of the transcriptionally repressed PHO5 gene of Saccharomyces cerevisiae. *Mol. Cell. Biol.* **6**, 2298-2304.

Cardozo, T., Totrov, M. and Abagyan, R. (1995). Homology modeling by the ICM method. *Proteins* **23**, 403-414.

Daly, T. M., Long, C. A. and Bergman, L. W. (2001). Interaction between two domains of the *P. yoelii* MSP-1 protein detected using the yeast two-hybrid system. *Mol. Biochem. Parasitol.* **117**, 27-35.

Dobrowolski, J. M. and Sibley, L. D. (1996). *Toxoplasma* invasion of mammalian cells is powered by the actin cytoskeleton of the parasite. *Cell* **84**, 933-939.

Dobrowolski, J. M., Carruthers, V. B. and Sibley, L. D. (1997a). Participation of myosin in gliding motility and host cell invasion by *Toxoplasma gondii*. *Mol. Microbiol.* **26**, 163-173.

Dobrowolski, J. M., Niesman, I. R. and Sibley, L. D. (1997b). Actin in the parasite *Toxoplasma gondii* is encoded by a single copy gene, ACT1 and exists primarily in a globular form. *Cell Motil. Cytoskeleton* **37**, 253-262.

Dominguez, R., Freyzon, Y., Trybus, K. M. and Cohen, C. (1998). Crystal structure of a vertebrate smooth muscle myosin motor domain and its complex with the essential light chain: visualization of the pre-power stroke state. *Cell* **94**, 559-571.

Folsch, H., Pypaert, M., Schu, P. and Mellman, I. (2001). Distribution and function of AP-1 clathrin adaptor complexes in polarized epithelial cells. *J. Cell Biol.* **152**, 595-606.

Heintzelman, M. B. and Schwartzman, J. D. (1997). A novel class of unconventional myosins from *Toxoplasma gondii*. *J. Mol. Biol.* **271**, 139-146.

Heintzelman, M. B. and Schwartzman, J. D. (1999). Characterization of Myosin-A and myosin-C: Two class XIV unconventional myosins from *Toxoplasma gondii*. *Cell Motil. Cytoskeleton* **44**, 58-67.

Herm-Gotz, A., Weiss, S., Stratmann, R., Fujita-Becker, S., Ruff, C., Meyhofer, E., Soldati, T., Manstein, D. J., Geeves, M. A. and Soldati, D. (2002). *Toxoplasma gondii* myosin A and its light chain: a fast, single-headed, plus-end-directed motor. *EMBO J.* **21**, 2149-2158.

Hettmann, C., Herm, A., Geiter, A., Frank, B., Schwarz, E., Soldati, T. and Soldati, D. (2000). A dibasic motif in the tail of a class XIV apicomplexan myosin is an essential determinant of plasma membrane localization. *Mol. Biol. Cell* **11**, 1385-1400.

Kappe, S., Bruderer, T., Gantt, S., Fujioka, H., Nussenzweig, V. and Ménard, R. (1999). Conservation of a Gliding Motility and Cell Invasion Machinery in Apicomplexan Parasites. *J. Cell Biol.* **147**, 937-944.

King, C. A. (1988). Cell motility of sporozoan protozoa. *Parasitol. Today* **4**, 315-319.

Kusakabe, T., Motoki, K. and Hori, K. (1997). Mode of interactions of human aldolase isozymes with cytoskeletons. *Arch. Biochem. Biophys.* **344**, 184-193.

Lewit-Bentley, A. and Rety, S. (2000). EF-hand calcium-binding proteins. *Curr. Opin. Struct. Biol.* **10**, 637-643.

Mann, T. and Beckers, C. (2001). Characterization of the subpellicular network, a filamentous membrane skeletal component in the parasite *Toxoplasma gondii*. *Mol. Biochem. Parasitol.* **115**, 257-268.

Margos, G., Siden-Kiamos, I., Fowler, R. E., Gillman, T. R., Spaccapelo, R., Lycett, G., Vlachou, D., Papagiannakis, G., Eling, W. M., Mitchell, G. H. et al. (2000). Myosin A expressions in sporogonic stages of *Plasmodium*. *Mol. Biochem. Parasitol.* **111**, 465-469.

Matuschewski, K., Mota, M. M., Pinder, J. C., Nussenzweig, V. and Kappe, S. H. (2001). Identification of the class XIV myosins Pb-MyoA and Py-MyoA and expression in *Plasmodium* sporozoites. *Mol. Biochem. Parasitol.* **112**, 157-161.

Matuschewski, K., Nunes, A. C., Nussenzweig, V. and Menard, R. (2002). *Plasmodium* sporozoite invasion into insect and mammalian cells is directed by the same dual binding system. *EMBO J.* **21**, 1597-1606.

Meis, J. F., Verhave, J. P., Jap, P. H. and Meuwissen, J. H. (1985). Transformation of sporozoites of *Plasmodium berghei* into exoerythrocytic forms in the liver of its mammalian host. *Cell Tissue Res.* **241**, 353-360.

Meissner, M., Schluter, D. and Soldati, D. (2002). Role of *Toxoplasma gondii* myosin A in powering parasite gliding and host cell invasion. *Science* **298**, 837-840.

Mermall, V., Post, P. L. and Mooseker, M. S. (1998). Unconventional myosins in cell movement, membrane traffic, and signal transduction. *Science* **279**, 527-533.

Mooseker, M. S. and Cheney, R. E. (1995). Unconventional myosins. *Annu. Rev. Cell Dev. Biol.* **11**, 633-675.

Morrissette, N. S., Murray, J. M. and Roos, D. S. (1997). Subpellicular microtubules associate with an intramembranous particle lattice in the protozoan parasite *Toxoplasma gondii*. *J. Cell Sci.* **110**, 35-42.

Nelson, M. R. and Chazin, W. J. (1998). Structures of EF-hand Ca(2+)-binding proteins: diversity in the organization, packing and response to Ca2+ binding. *Biometals* **11**, 297-318.

Nussenzweig, V. and Nussenzweig, R. S. (1985). Circumsporozoite proteins of malaria parasites. *Cell* **42**, 401-403.

Pinder, J. C., Fowler, R. E., Bannister, L. H., Dluzewski, A. R. and Mitchell, G. H. (2000). Motile systems in malaria merozoites: how is the red blood cell invaded? *Parasitol. Today* **16**, 240-245.

Pinder, J. C., Fowler, R. E., Dluzewski, A. R., Bannister, L. H., Lavin, F.

M., Mitchell, G. H., Wilson, R. J. and Gratzer, W. B. (1998). Actomyosin motor in the merozoite of the malaria parasite, *Plasmodium falciparum*: implications for red cell invasion. *J. Cell Sci.* **111**, 1831-1839.

Poupel, O. and Tardieux, I. (1999). *Toxoplasma gondii* motility and host cell invasiveness are drastically impaired by jasplakinolide, a cyclic peptide stabilizing F-actin. *Microbes Infect.* **1**, 653-662.

Russell, D. G. (1983). Host cell invasion by Apicomplexa: an expression of the parasite's contractile system? *Parasitology* **87**, 199-209.

Russell, D. G. and Sinden, R. E. (1981). The role of the cytoskeleton in the motility of coccidian sporozoites. *J. Cell Sci.* **50**, 345-359.

Schindler, R., Weichselsdorfer, E., Wagner, O. and Bereiter-Hahn, J. (2001). Aldolase-localization in cultured cells: cell-type and substrate- specific regulation of cytoskeletal associations. *Biochem. Cell Biol.* **79**, 719-728.

Shaw, M. K. and Tilney, L. G. (1999). Induction of an acrosomal process in *Toxoplasma gondii*: visualization of actin filaments in a protozoan parasite. *Proc. Natl. Acad. Sci. USA* **96**, 9095-9099.

Sibley, L. D., Hakansson, S. and Carruthers, V. B. (1998). Gliding motility: an efficient mechanism for cell penetration. *Curr. Biol.* **8**, R12-R14.

Smith, D. B. and Johnson, K. S. (1988). Single-step purification of polypeptides expressed in *Escherichia coli* as fusions with glutathione S-transferase. *Gene* **67**, 31-40.

Sultan, A. A., Thathy, V., Frevert, U., Robson, K. J., Crisanti, A., Nussenzweig, V., Nussenzweig, R. S. and Ménard, R. (1997). TRAP is necessary for gliding motility and infectivity of *Plasmodium* sporozoites. *Cell* **90**, 511-522.

Trottein, F., Triglia, T. and Cowman, A. F. (1995). Molecular cloning of a gene from *Plasmodium falciparum* that codes for a protein sharing motifs found in adhesive molecules from mammals and plasmodia. *Mol. Biochem. Parasitol.* **74**, 129-141.

Tsuji, M., Mattei, D., Nussenzweig, R. S., Eichinger, D. and Zavala, F. (1994). Demonstration of heat-shock protein 70 in the sporozoite stage of malaria parasites. *Parasitol. Res.* **80**, 16-21.

Wan, K. L., Carruthers, V. B., Sibley, L. D. and Ajioka, J. W. (1997). Molecular characterisation of an expressed sequence tag locus of *Toxoplasma gondii* encoding the micronemal protein MIC2. *Mol. Biochem. Parasitol.* **84**, 203-214.